Coherence Analysis using Canonical Coordinate Decomposition with Applications to Sparse Processing and Optimal Array Deployment

Mahmood R. Azimi-Sadjadi*[a], Ali Pezeshki[b] †, and Robert Wade[c]

[a]Information System Technologies, Inc, Fort Collins, CO.
[b]Colorado State University, Fort Collins, CO.
[c]US Army TACOM-ARDEC, Picatinny Arsenal, NJ.

ABSTRACT

Sparse array processing methods are typically used to improve the spatial resolution of sensor arrays for the estimation of direction of arrival (DOA). The fundamental assumption behind these methods is that signals that are received by the sparse sensors (or a group of sensors) are coherent. However, coherence may vary significantly with the changes in environmental, terrain, and, operating conditions. In this paper canonical correlation analysis is used to study the variations in coherence between pairs of sub-arrays in a sparse array problem. The data set for this study is a subset of an acoustic signature data set, acquired from the US Army TACOM-ARDEC, Picatinny Arsenal, NJ. This data set is collected using three wagon-wheel type arrays with five microphones. The results show that in nominal operating conditions, i.e. no extreme wind noise or masking effects by trees, building, etc., the signals collected at different sensor arrays are indeed coherent even at distant node separation.

Keywords: DOA estimation, sparse sensor arrays, signal coherence, canonical coordinates.

1. INTRODUCTION

Unattended passive acoustic sensors are widely used for remote battlefield surveillance, situation awareness and monitoring applications[1]-.[4] These small and cost effective sensors can provide real-time information about different types of ground and airborne targets. They are rugged and reliable and can be left in the field for a long period of time after deployment. Generally, there can be a wide variety of target types in battlefield depending on the specific mission, e.g. troops, ground targets (trucks, tanks, etc), airborne targets (helicopters, missiles, airplanes) with signatures that overlap both spectrally and temporally. Unfortunately, the existing DOA estimation algorithms have limited capability when applied to realistic multiple target scenarios, especially when the targets are spatially close together and move in tight staggered, abreast or single-file formations. Additionally, optimum performance is highly dependent on terrain, weather, and background noise estimates.

The spatial resolution may be improved by exploiting sparse array configurations[5]-.[7] However, the fundamental requirement for sparse processing is that signals received at different sensors or sensory nodes are coherent. Loss of signal coherence would have a dramatic impact on the accuracy of the DOA estimation, as well as the ability to detect, track, and resolve multiple targets. There are many factors that may impact signal coherence. The signal coherence depends on the distance between the sensor sub-arrays in the sparse configuration. Variations in environmental, terrain, and operating conditions such as wind and presence of natural or man-made obstacles also impact the signal coherence.

Thus in order to successfully employ sparse array processing methods, or deploy ground sensor arrays, it is essential to analyze the variations in signal coherence with respect to the aforementioned factors. In this paper, canonical correlation analysis (CCA),[8][9] is used to study the variations in coherence between sub-arrays of sensors in a sparse array configuration. CCA provides an elegant framework for analyzing linear dependence (coherence) between two data channels (sensory nodes). It decomposes the linear dependence between the channels into the

*mo@infsyst.biz; phone: 1 970 224 2556; fax 1 970 224 2556
†A. Pezeshki is a consultant at Information System Technologies, Inc.

linear dependence between the canonical coordinates of the channels, and this linear dependence is determined by the corresponding canonical correlations.[9] The data set for this study is a subset of an acoustic signature database, acquired from the US Army TACOM-ARDEC, Picatinny Arsenal, NJ. This data set is collected using three wagon-wheel type arrays with five microphones. The results show that in nominal operating conditions, i.e. no extreme wind noise or masking effects by trees, building, etc., the signals collected at different sensor arrays are indeed coherent even at distant node separation.

2. A REVIEW ON CANONICAL COORDINATE DECOMPOSITION

Consider the two-channel data, $\mathbf{x} \in R^{m\times 1}$ and $\mathbf{y} \in R^{n\times 1}$ with m being the smaller dimension ($m \le n$). Assume that $\mathbf{x}$ and $\mathbf{y}$ have zero means and share the composite covariance matrix

$$\begin{bmatrix} \mathrm{R}_{xx} & \mathrm{R}_{xy} \\ \mathrm{R}_{yx} & \mathrm{R}_{yy} \end{bmatrix} = E\left[\begin{pmatrix} \mathbf{x} \\ \mathbf{y} \end{pmatrix} \begin{pmatrix} \mathbf{x}^T & \mathbf{y}^T \end{pmatrix} \right] \tag{1}$$

We may write the singular value decomposition (SVD) of the coherence matrix, C, as[9]

$$\begin{aligned} \mathrm{C} = \mathrm{R}_{xx}^{-1/2}\mathrm{R}_{xy}\mathrm{R}_{yy}^{-T/2} = \mathrm{FKG}^T \quad \text{and} \quad \mathrm{F}^T\mathrm{CG} = \mathrm{K}, \\ \mathrm{F}^T\mathrm{F} = \mathrm{I}, \;\; \mathrm{G}^T\mathrm{G} = \mathrm{I}, \quad \mathrm{K} = \mathrm{diag}[k_1, k_2, \ldots, k_m]; \end{aligned} \tag{2}$$

where $\mathrm{R}_{xx}^{-1/2}\mathrm{R}_{xx}\mathrm{R}_{xx}^{-T/2} = \mathrm{I}$, and $\mathrm{R}_{xx}^{1/2}\mathrm{R}_{xx}^{T/2} = \mathrm{R}_{xx}$. We note that only nonzero singular values of C and their corresponding singular vectors are considered in this SVD.

Then, the canonical coordinates of $\mathbf{x}$ and $\mathbf{y}$ are defined as[9]

$$\begin{bmatrix} \mathbf{u} \\ \mathbf{v} \end{bmatrix} = \begin{bmatrix} \mathrm{F}^T & 0 \\ 0 & \mathrm{G}^T \end{bmatrix} \begin{bmatrix} \mathrm{R}_{xx}^{-1/2} & 0 \\ 0 & \mathrm{R}_{yy}^{-1/2} \end{bmatrix} \begin{bmatrix} \mathbf{x} \\ \mathbf{y} \end{bmatrix} \tag{3}$$

where the elements of $\mathbf{u}$ and $\mathbf{v}$ are the canonical coordinates of $\mathbf{x}$ and $\mathbf{y}$ respectively.

These canonical coordinates share the composite covariance matrix

$$E\left[\begin{pmatrix} \mathbf{u} \\ \mathbf{v} \end{pmatrix} \begin{pmatrix} \mathbf{u}^T & \mathbf{v}^T \end{pmatrix} \right] = \begin{bmatrix} \mathrm{I} & \mathrm{K} \\ \mathrm{K}^T & \mathrm{I} \end{bmatrix} \tag{4}$$

The diagonal cross-covariance matrix

$$\mathrm{K} = \mathrm{F}^T\mathrm{CG} = \mathrm{R}_{uv} \tag{5}$$

is the canonical correlation matrix of canonical correlations k_i; $i = 1, 2, \ldots, m$, with $1 \ge k_1 \ge k_2 \ge \cdots \ge k_m > 0$.[9] The interpretation of (4) is that canonical coordinates $\mathbf{u}$ and $\mathbf{v}$ are individually white, i.e. $E[u_i u_j] = \delta(k-l)$ and $E[v_i v_j] = \delta(i-j)$, and only cross-correlated in pairs, i.e $E[u_i v_j] = k_i\delta(i-j)$. This decomposition packs the linear dependence or coherence between $\mathbf{x}$ and $\mathbf{y}$ into the linear dependence between pairs of corresponding canonical coordinates.

The standard measure of linear dependence for the composite vector $\mathbf{z} = [\mathbf{x}^T \;\; \mathbf{y}^T]^T$ is the Hadamard ratio, which satisfies the inequality[9]

$$0 \le \frac{\det\{\mathrm{R}_{zz}\}}{\prod_{i=1}^{m+n}(\mathrm{R}_{zz})_{ii}} \le 1 \tag{6}$$

where $(\mathrm{R}_{zz})_{ii}$'s are the diagonal elements of R_{zz}. The ratio takes the value 0 iff there is linear dependence among elements of $\mathbf{z}$; it takes the value 1 iff elements of $\mathbf{z}$ are mutually uncorrelated. It may be shown that the Hadamard ratio in (6) has a decomposition of form[9]

$$\frac{\det\{\mathrm{R}_{zz}\}}{\prod_{i=1}^{m+n}(\mathrm{R}_{zz})_{ii}} = \frac{\det\{\mathrm{R}_{xx}\}}{\prod_{i=1}^{m}(\mathrm{R}_{xx})_{ii}} \det\{\mathrm{I} - \mathrm{KK}^T\} \frac{\det\{\mathrm{R}_{yy}\}}{\prod_{i=1}^{n'}(\mathrm{R}_{yy})_{ii}} \tag{7}$$

The first term on the right hand side measures the linear dependence *among* the elements of $\mathbf{x}$, and the third term measures the linear dependence *among* the elements of $\mathbf{y}$. The middle term

$$L = \det\{\mathrm{I} - \mathrm{K}\mathrm{K}^T\} = \prod_{i=1}^{m}(1 - k_i^2); \quad 0 \leq L \leq 1 \tag{8}$$

measures the linear dependence *between* elements of $\mathbf{x}$ and $\mathbf{y}$. The ith term of the product on the right hand side of (8), i.e. $(1 - k_i^2)$, measures the linear dependence between the ith canonical coordinate pair (u_i, v_i).[9] Thus, the linear dependence between $\mathbf{x}$ and $\mathbf{y}$ is decomposed into the linear dependence between their canonical coordinates, and this linear dependence is determined by the corresponding canonical correlations.

Correspondingly,

$$H = 1 - L = 1 - \det\{\mathrm{I} - \mathrm{K}\mathrm{K}^T\} = 1 - \prod_{i=1}^{m}(1 - k_i^2); \quad 0 \leq H \leq 1 \tag{9}$$

measures the similarity or coherence between the elements of $\mathbf{x}$ and $\mathbf{y}$. The coherence measure H takes the value 1 iff elements of $\mathbf{x}$ and $\mathbf{y}$ are coherent; it takes the value 0 iff elements of $\mathbf{x}$ and $\mathbf{y}$ are incoherent or mutually uncorrelated.[9]

3. DATA SET

The data set for this study is a subset of an acoustic signature database acquired from the US Army TACOM-ARDEC, Picatinny Arsenal, NJ. The data has been collected using three wagon wheel-type pattern array of five identical elements (microphones) with 2ft radius at a sampling rate of $f_s = 1024$Hz. Table 1 shows the distances between the three sensory nodes. The acoustic signature database contains several runs for different single-file formations. The runs consist of acoustic signatures of one or more vehicles of four typical classes, namely wheeled vs tracked and heavy vs light. In this paper, we use the data of two runs that contain only one moving vehicle in order to easily analyze the variations in coherence with respect to environmental conditions and distance between the sparse arrays.

The first run contains a single light tracked vehicle and has been collected in relatively strong wind. The spectrograms of the center microphones of the three sensory nodes for this runs are shown in Figure 1. As can be observed the effects of wind noise is clearly evident in these spectrograms, especially in the beginning and end of the data collection period. The second run, on the other hand, has been collected in mild wind condition, and contains one moving and one stationary target. The moving target is a heavy wheeled vehicle. The stationary target is located approximately 8 km away from the nodes and hence is not detected by any of the nodes. The spectrogram of the center microphones of the nodes for this run are shown in Figure 2. Unlike the first run the source indications are clear and strong and wind noise effects are minimal.

In order to account for the errors caused by differences between the nominal values of array parameters, namely gain, phase, and sensor positions, and the values of these parameters after the array is deployed, the data must be calibrated prior to coherence analysis. The time series recorded by each microphone is first filtered using a sliding Hamming window of size 2048 (corresponding to 2 seconds of data) with 50% overlap. The calibration is then performed on each 2048 samples for the frequency range of 50-250Hz. The reason for not considering frequencies higher than 250Hz is that the aliasing frequency for the array is approximately 277Hz.

Table 1. Distances between the sensory nodes.

	Node 1	Node 2	Node 3
Node 1	–	531.20	589.48
Node 2	531.20	–	584.86
Node 3	589.48	584.86	–

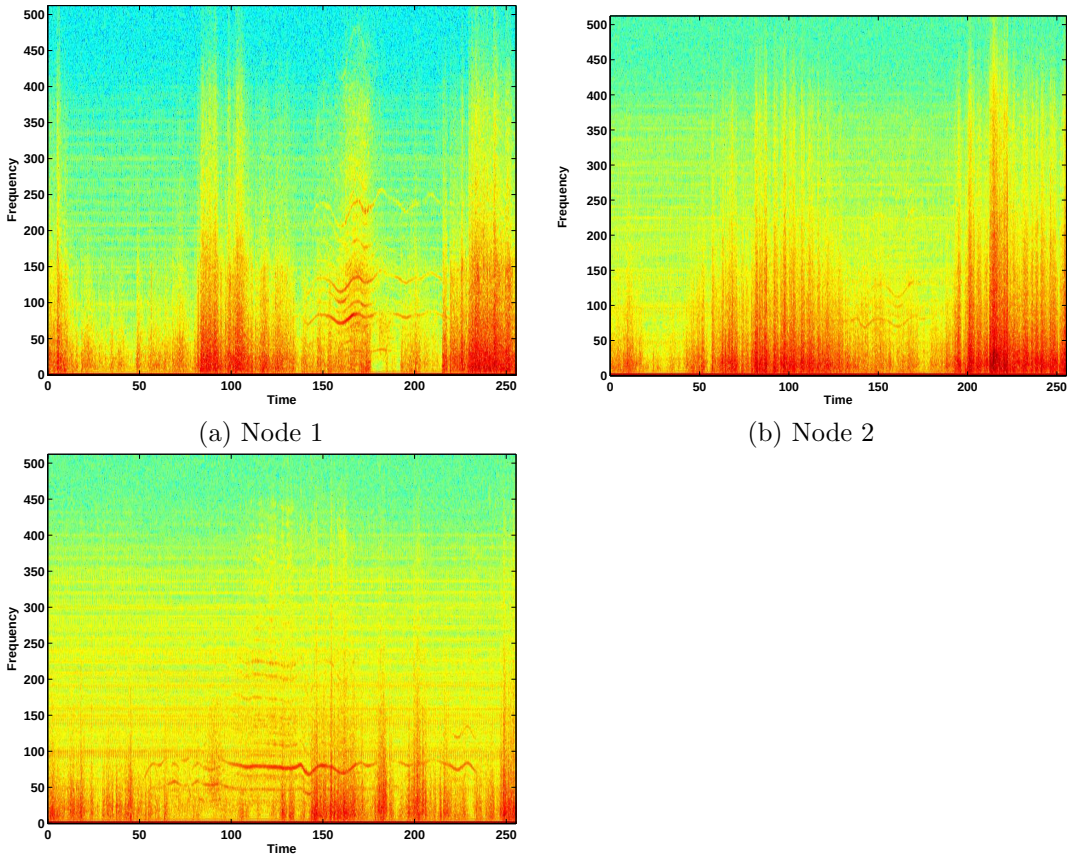

(a) Node 1

(b) Node 2

(c) Node 3

Figure 1. Spectrograms of the center microphones of the three nodes for the first run. The target is a light tracked vehicle.

4. COHERENCE ANALYSIS PROCEDURE

In order to use canonical correlation analysis to measure signal coherence in our problem, let us consider the scenario depicted in Figure 3. At every point, each node records an $L \times 1$ data vector, where L corresponds to the number of sensory elements in each sensor array node. For our data set, since there are five microphones in each array, $L = 5$. During the time interval $[t_1, t_2]$ the data collected by each node form an $L \times N$; $N = (t_2 - t_1)f_s$, data matrix (see the magnified figure of Node 1). To measure the coherence between the ith and jth nodes, using canonical correlation analysis, the $L \times N$ data matrices collected by the ith and jth nodes may be considered as the ensemble sets for the $\mathbf{x}$ and $\mathbf{y}$-channels, respectively. The linear coherence between the nodes may then be computed using (9). In the experiments to be presented, the time interval $t_2 - t_1$ is chosen to be $t_2 - t_1 = 0.125sec.$ Thus, at every 0.125 second the coherence analysis is carried out between two sensory nodes. To smooth out sharp transitions in values of coherence in every computational period of 0.125 second a moving average filter of order 16 may be applied to the values of coherence.

5. EXPERIMENTAL RESULTS

Figures 4(a)-(c) show the plots of coherence vs. time for the three possible pairwise combination of the nodes of the first data set (first run) explained earlier. The range of the source from each node in the pair is plotted in Figures 5(a)-(c) for the same node combinations. By looking at the coherence plots in Figure 4 and the spectrograms in Figure 1, it can be seen that the linear coherence between the pairs of nodes is reduced in time intervals where the wind noise is dominant and the recorded signal in one of the nodes does not exhibit

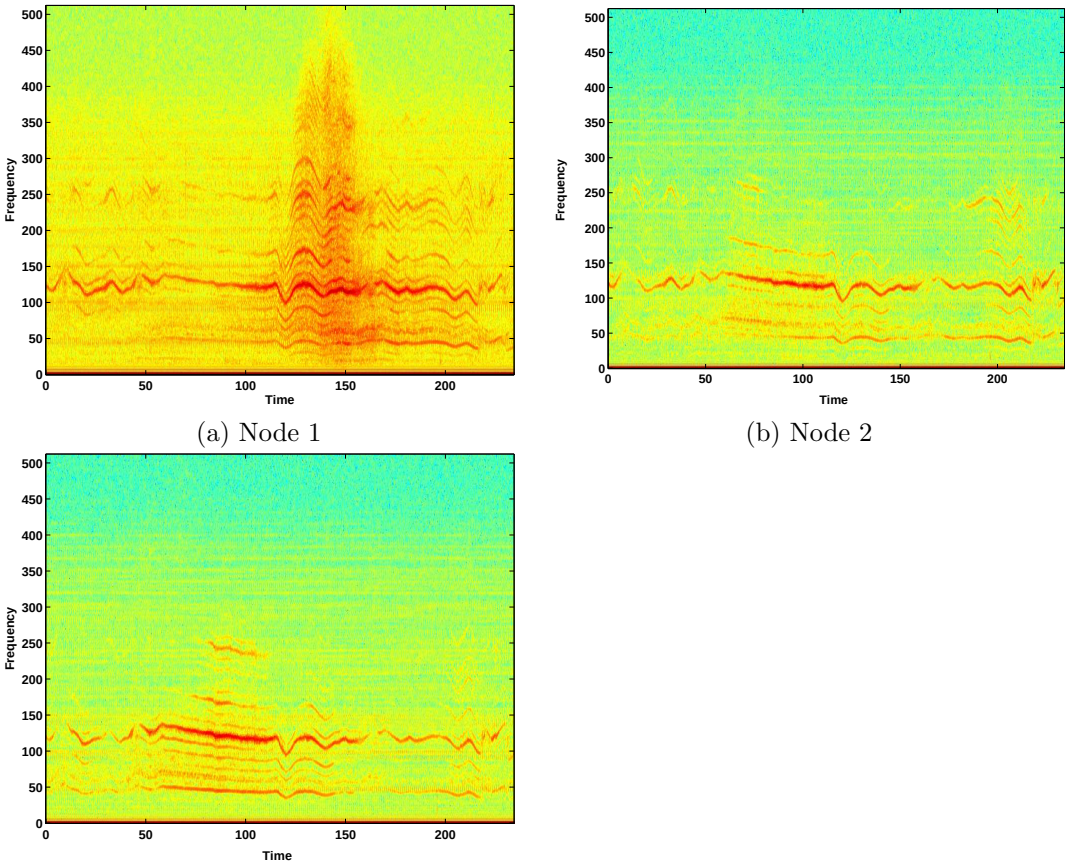

(a) Node 1

(b) Node 2

(c) Node 3

Figure 2. Spectrograms of the center microphones of the three nodes for the second run. The target is a heavy wheeled vehicle.

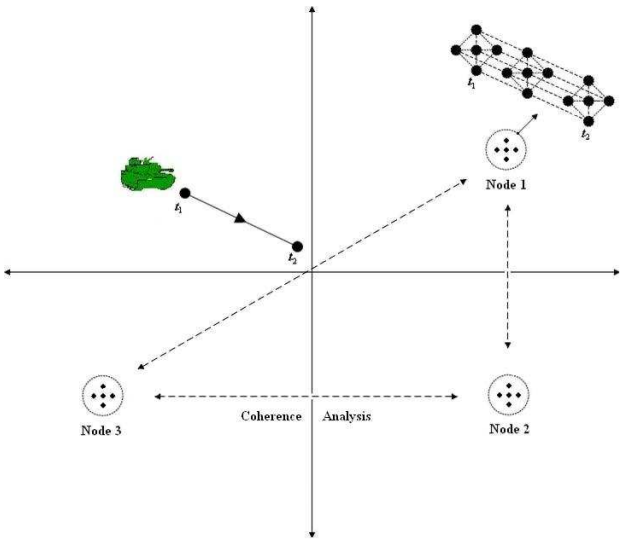

Figure 3. Coherence analysis between sensory nodes.

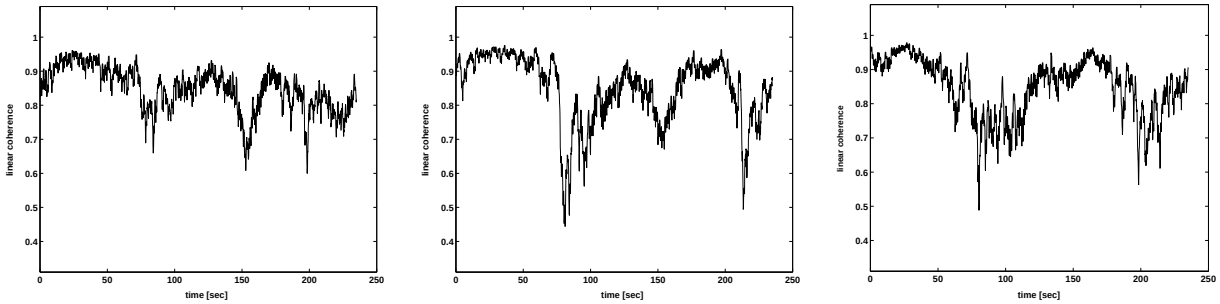

(a) (b) (c)

Figure 4. Plots of coherence between pairwise combinations of the nodes for the data of the first run. Linear coherence between (a) nodes 1 and 2, (b) nodes 1 and 3, and (c) nodes 2 and 3.

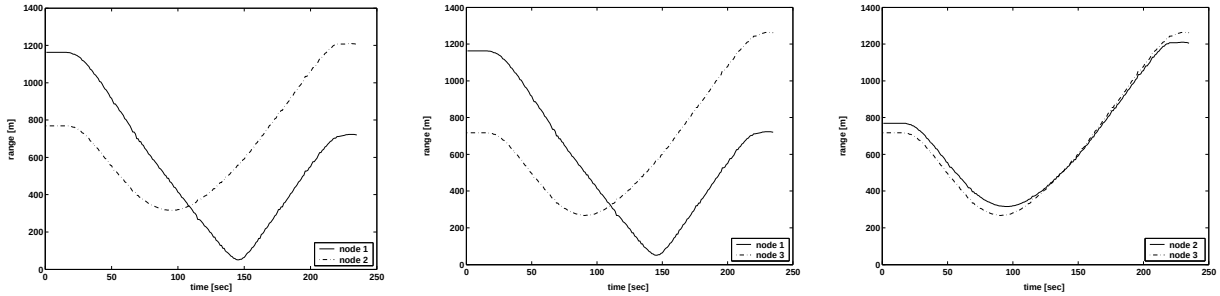

(a) (b) (c)

Figure 5. Range of the target to the three sensory nodes in the data of the first run; (a) nodes 1 and 2, (b) nodes 1 and 3, and (c) nodes 2 and 3.

strong target indications. For example consider the coherence between nodes 1 and 3 (Figure 4(b)) and the corresponding spectrograms (Figures 1(a) and (c)) at the time interval of 80 to 90 sec. As evident, the coherence has dropped from approximately 0.95 to 0.45. However, except for the cases where wind noise is reducing the coherence, the signals received by the nodes are indeed coherent, despite the fact that the nodes are approximately $500m$ to $600m$ apart.

For the second data set (second run), the coherence plots between pairwise combination of the nodes are shown in Figures 6(a)-(c) for nodes 1 and 2, nodes 1 and 3, and nodes 2 and 3, respectively. The range of the source from each node in the pair is plotted in Figures 7(a)-(c). It is seen that the coherence between the nodes in Figure 6 is close to 1 almost everywhere, for all three cases. This is due to the fact that the wind noise is minimal in this case and the target indications are strong at almost every snapshot. However, looking at the coherence plots for nodes 1 and 2 (Figure 6(a)), and nodes 1 and 3 (Figure 6(b)), one can see a sudden drop in coherence in approximately 140 to 150 sec time interval. Since this occurs only in the two cases that involve node 1, it suggests that the loss of coherence is due to some property in the recorded signal of node 1. A close look at the spectrogram of the center microphone of node 1 in Figure 2(a) reveals that at the time period of 140 to 150 sec source indication is very strong, but may be too strong to cause saturation. By looking at the range plot in Figure 6(a), we see that the time interval 140 to 150 corresponds to the closest point of approach (CPA) of the target to node 1. However, since the source is still far from nodes 2 and 3, this extremely strong target indication is not seen by these nodes, hence causing a significant drop in coherence. Nonetheless, except for this small time interval, the signals received by the three nodes are indeed coherent, despite the fact that the nodes are approximately $500m$ to $600m$ apart. For nodes 2 and 3, near perfect coherence is observed at all times.

It is also interesting to note the pattern of coherence at the beginning and the end of the runs. In all the cases studied, at the end of the track, where the target starts decelerating the coherence between the nodes shows a

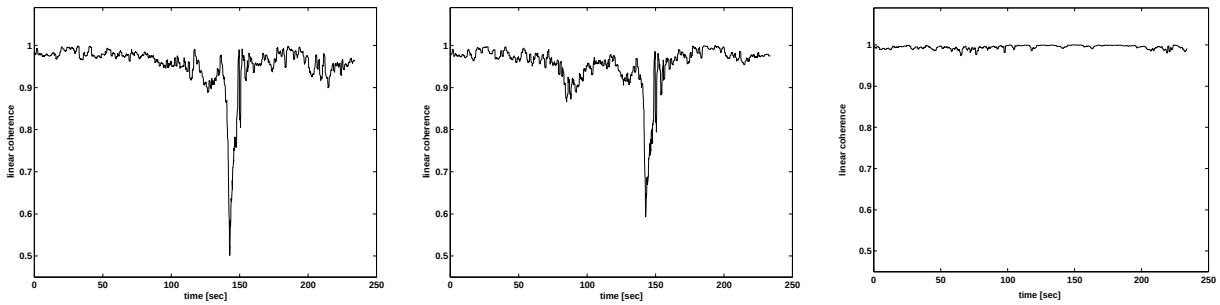

Figure 6. Plots of coherence between pairwise combinations of the nodes for the data of the second run. Linear coherence between (a) nodes 1 and 2, (b) nodes 1 and 3, and (c) nodes 2 and 3.

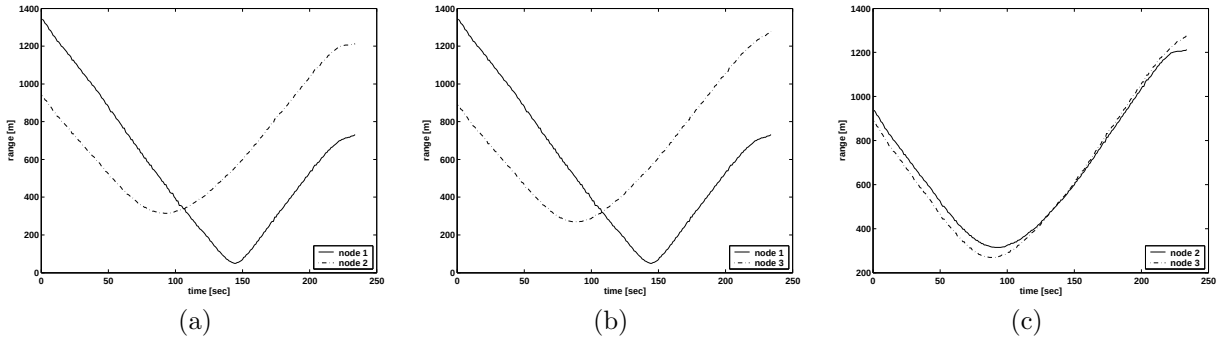

Figure 7. Range of the target to the three sensory nodes in the data of the second run. (a) Nodes 1 and 2, (b) nodes 1 and 3, and (c) nodes 2 and 3.

sudden decrease. However, after a few seconds the coherence increases again. This is due to the fact that the onset of deceleration of the source is observed by the sensory nodes with a time difference that corresponds to the relative delay between the nodes. Once the target is no longer moving and adequate time is elapsed, the coherence increases again. A similar argument can be made to explain the coherence pattern at the beginning of the track, i.e. early stages of coherence plot. At the beginning of the track, the source is stationary hence leading to high coherence. However, when the target starts accelerating, due to the relative time delay of the nodes the coherence decreases hence producing a peak in the plot at the time of acceleration.

6. CONCLUSION AND FUTURE WORK

In this paper, canonical correlation analysis has been used to measure the signal coherence between pairs of sparse sensor arrays. The reason for using canonical coordinates is that they provide an elegant framework for analysis of coherence between two data channels as they decompose the coherence between the channels into the coherence between the canonical coordinates of the channels. This decomposition provide us with a power tool for analysis of coherence between pairs of sparse sensor arrays. In our experiments the sparse sensor arrays were deployed in a triangular formation with approximate pairwise distances of 480 to 600 meters. The results indicate that in nominal operating conditions, i.e. no extreme wind noise or masking by trees, building, etc., the signals collected at different sensor arrays are indeed coherent even at distant node separation (600m). This suggests the possibility of exploiting sparse array processing for DOA estimation for the data set under study.

The two-channel coherence analysis method used here may also be used to identify two groups of arbitrary deployed sensors that exhibit high pair-wise coherence. This is useful in situations where the sensor arrays are replaced by a modest quantity of inexpensive single microphones. The method offers the capability to

form dynamic space-time varying sensory arrays that can offer better localization and tracking performance in multi-formation/multi-target scenarios.

ACKNOWLEDGMENTS

This work is funded by Army SBIR-Phase II contract # DAAE30-03-C-1055. The data and technical support has been provided by the US Army TACOM-ARDEC, Picatinny Arsenal, NJ. The authors would like to thank Myron Hohil for his invaluable suggestions and technical support.

REFERENCES

1. N. Srour, "Unattended ground sensors- a prospective for operational needs and requirements," *Technical Report prepared for NATO* , Army Research Lab, Oct. 1999.
2. T. Pham and M. Fong, "Real-time implementation of music for wideband acoustic detection and tracking," *Proc. of SPIE AeroSense'97: Automatic Target Recognition VII* , Oct. 1997.
3. T. Pham and B. M. Sadler, "Wideband array processing algorithms for acoustic tracking of ground vehicles," *Technical Report* , Army Research Lab, Adelphi, MD, 1997.
4. M. R. Azimi-Sadjadi, "Detection, tracking and classification of multiple targets using advanced beamforming and classification methods," *Summary Report, Phase II SBIR-Army* , Information System Technologies Inc., Jan. 2004.
5. K. T. Wong and M. D. Zoltowski, "Direction finding with sparse rectangular dual-size spatial invariance array," *IEEE Trans. on Aerospace Electrn. Syst.* **34**, pp. 1320–1327, Oct. 1998.
6. M. D. Zoltowski and K. T. Wong, "Esprit-based 2-d direction-finding with a sparse uniform array of electromagnetic vector-sensors," *IEEE Trans. on Signal Processing* **48**, pp. 2195–2204, Aug. 2000.
7. M. D. Zoltowski and K. T. Wong, "Closed-form eigenstructure-based direction finding using arbitrary but identical subarrays on a sparse uniform cartesian array grid," *IEEE Trans. on Signal Processing* **48**, pp. 2205–2210, Aug. 2000.
8. H. Hotelling, "Relation between two sets of variates," *Biometrica* **28**, pp. 321–377, 1936.
9. L. L. Scharf and C. T. Mullis, "Canonical coordinates and the geometry of inference, rate and capacity," *IEEE Trans. on Signal Processing* **48**, pp. 824–831, March 2000.